Water Research X 27 (2025) 100312

Contents lists available at ScienceDirect

Water Research X

journal homepage: www.sciencedirect.com/journal/water-research-x

Dual role of organic matter in Feammox-driven nitrogen and phosphate removal

Yi Liu [a], Jiachen Dong [a], Xiaohui Cheng [a], Xiaotong Cen [b], Yan Dang [a], Kangning Xu [a,*], Min Zheng [b,*]

[a] Beijing Key Lab for Source Control Technology of Water Pollution, College of Environmental Science and Engineering, Beijing Forestry University, Beijing 100083, China
[b] Water Research Centre, School of Civil and Environmental Engineering, University of New South Wales, Sydney, New South Wales 2052, Australia

ARTICLE INFO

Keywords:
Feammox
Autotrophic nitrogen removal
Organic matter
Vivianite
Iron cycle

ABSTRACT

Feammox is a novel microbial process that enables simultaneous nitrogen and phosphorus removal in wastewater treatment. This study investigated the role of organic matter in Feammox-driven nutrient removal during long-term bioreactor operation by gradually increasing the influent chemical oxygen demand (COD) concentration from 0 to 50, and then to 100 mg/L. The results revealed that the ammonium removal efficiency was reduced from 60.5 % to 20.7 % with COD concentration increasing from 0 to 100 mg/L. In contrast, organic matter enhanced nitrate removal through heterotrophic denitrification, which outcompeted nitrate-dependent Fe(II) oxidation. Phosphorus removal was increased up to approximately 90 % via Fe(II)-mediated precipitation, forming vivianite crystals, evidenced by X-ray diffraction analysis. Continuous addition of Fe(III) alleviated the inhibitory effect of organic matter on ammonia oxidation by serving as an alternative electron acceptor, reducing competition. Therefore, optimizing organic matter levels and ensuring sufficient Fe(III) availability are crucial for achieving efficient nutrient removal in Feammox systems, particularly for treating wastewater with a low carbon/nitrogen ratio.

1. Introduction

Feammox (ferric iron-mediated anaerobic ammonium oxidation) is a microbial process that utilizes ferric ion (Fe(III)) as an electron acceptor to oxidize ammonia into nitrogen gas (N_2) as the primary nitrogen product under anaerobic conditions. Minor amounts of nitrite (NO_2^-) and nitrate (NO_3^-) are also produced (Eqs. (1)–(3)) (Clément et al., 2005; Ding et al., 2017, 2014; Yang et al., 2012). Compared to traditional nitrogen removal processes such as nitrification-denitrification, shortcut nitrification-denitrification, and partial nitrification-anammox (Zhen et al., 2024), Feammox does not require aeration or organic carbon for nitrogen removal (Cheng et al., 2025), potentially contributing to zero nitrous oxide (N_2O) emissions (Zheng et al., 2025). This suggests that Feammox could represent a novel autotrophic nitrogen removal pathway for wastewater, potentially offering significant energy and carbon savings.

$$3Fe(OH)_3 + 5H^+ + NH_4^+ \rightarrow 3Fe^{2+} + 9H_2O + 0.5N_2 \quad \Delta_r G_m = -245 kJ/mol \tag{1}$$

$$6Fe(OH)_3 + 10H^+ + NH_4^+ \rightarrow 6Fe^{2+} + 16H_2O + NO_2^- \quad \Delta_r G_m = -164 kJ/mol \tag{2}$$

$$8Fe(OH)_3 + 14H^+ + NH_4^+ \rightarrow 8Fe^{2+} + 21H_2O + NO_3^- \quad \Delta_r G_m = -207 kJ/mol \tag{3}$$

Feammox has demonstrated high ammonia removal efficiencies in treating concentrations of 50–100 mg N/L (Cheng et al., 2025).To initiate Feammox, two types of inoculated sludge have been reported: (1) anaerobically digested or activated sludge rich in organic matter, along with a high iron dosage (Yang et al., 2018; Zhu et al., 2022); and (2) anammox sludge, an autotrophic nitrogen removal process with low organic matter content (Cheng et al., 2025; Li et al., 2018). Interestingly, Feammox reactors inoculated with anammox sludge require a significantly less iron compared to a theoretical value based on stoichiometric calculations (Cheng et al., 2025; Hu et al., 2022), potentially further reducing operational costs and carbon emissions.

Most studies to date have focused on Feammox for nitrogen removal using synthetic wastewater devoid of organic matter. However, in

* Corresponding authors.
E-mail addresses: xukangning@bjfu.edu.cn (K. Xu), min.zheng1@unsw.edu.au (M. Zheng).

https://doi.org/10.1016/j.wroa.2025.100312
Received 15 December 2024; Received in revised form 26 January 2025; Accepted 2 February 2025
Available online 4 February 2025

practical applications, organic matter is ubiquitous in wastewater, and its impact on Feammox remains poorly understood. It is hypothesized that organic matter in wastewater may have serval impacts on Feammox-driven nitrogen and phosphorus removal:

1) Organic matter could inhibit Feammox, as observed in anammox systems (Ma et al., 2022; Nguyen et al., 2023; Zhu et al., 2022). Indeed, recent studies have shown that appropriate concentration of organic matter reduced the ammonia removal efficiency in Feammox. Yet, one study still reported enhanced nitrogen removal performance with slightly increased chemical oxygen demand (COD) concentration from 120 mg/L to 160 mg/L in a hydrogel Feammox bioreactor (Liang et al., 2023).
2) Organic matter may initiate competition for nitrite and nitrate, which are also the intermediates in nitrate-dependent ferrous oxidation (NDFO), a process associated with Feammox (Xing et al., 2018). NDFO process uses ferrous ion (Fe(II)) as an electron donor, serving as a substitute for organic matter to achieve nitrate reduction (Struab et al., 1996). It affects the pathway of ammonia oxidation through Feammox, as well as the cycle of iron reduction and oxidation. Organic matter could eliminate nitrate formed in Feammox due to heterotrophic denitrification (Nguyen et al., 2023). This indicates that the ammonia removal and the iron cycle might be influenced because of the competition between heterotrophic denitrification and NDFO.
3) Organic matter may stimulate heterotrophic dissimilatory iron reduction (to Fe(II)), increasing Fe(II) availability for vivianite (ferrous phosphate octahydrate) formation and potentially enhancing phosphorus removal (Wang et al., 2024).

This study aims to investigate performance of nitrogen and phosphorus removal and microbial response in the Feammox-driven wastewater treatment process under elevated organic matter concentrations, and to elucidate the critical role of organic matter in enhanced nitrogen and phosphorus removal. We operated a laboratory Feammox reactor for one year (Figure S1), progressively increasing influent acetate concentrations from 0 to 100 mg COD/L. The microbial community were analysed by 16S rRNA gene amplicon sequencing to examine the potential functional microorganisms. Moreover, the properties of the Feammox sludge were analysed to evaluate the oxidation and reduction of iron, as well as the removal mechanism of phosphate. Additionally, *ex-situ* batch experiments were conducted to explore the interactions between dissimilatory iron reduction and autotrophic NDFO in nitrate removal. Our findings provide critical insights into the role of organic matter in Feammox and its potential applications in wastewater treatment.

2. Results

2.1. Performance of Feammox reactor in the presence of organic matter

The Feammox reactor operated across three stages: stage I (0 mg/L COD), stage II (50 mg/L COD), and stage III (100 mg/L COD). stage III was divided into III-A and III-B due to significant iron re-dosing. Effluent nitrogen, phosphorus, COD, and iron concentrations are shown in Fig. 1.

The effluent ammonium concentration ranged from 16.0 to 22.5 mg N/L when no acetate was present in the influent (Fig. 1a), corresponding to an average ammonia removal efficiency of 60.5 ± 3.6 % (Fig. S2). However, the addition of organic matter in the influent, resulting in a COD concentration of 50 mg/L (C/N ratio of 1), significantly ($p < 0.01$) reduced the ammonia removal efficiency to 55.7 % ± 6.8 %. This efficiency further dropped to an average of just 20.7 % when the influent COD concentration increased to 100 mg/L (C/N ratio of 2). These results indicate that organic matter substantially inhibited ammonia oxidation

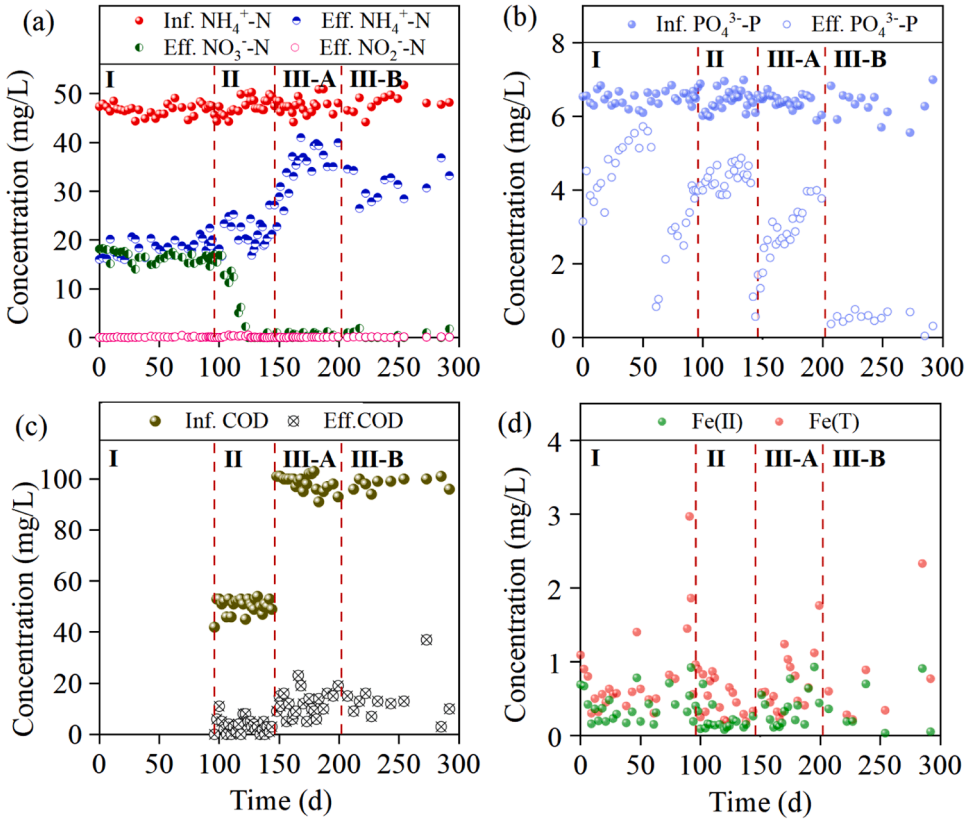

Fig. 1. Long-term changes in concentrations of nitrogen (a), phosphate (b), COD (c), and iron (d) during the Feammox reactor operation across three phases: stage I (Day 0–95), stage II (Day 96–145), and stage III (III-A Day 146–201, III-B Day 202–292).

in the Feammox bioreactor.

To address this, 20 mM amorphous FeOOH was added to the reactor on Day 202 during stage III. Following this addition, the effluent ammonium concentration decreased from 40.0 mg N/L on Day 199 to 26.5 mg N/L on Day 230 (Fig. 1a), suggesting that the iron source partially alleviated the inhibitory effects of organic matter. However, after Day 230, the effluent ammonium concentration gradually increased again, reaching 33.6 mg N/L by Day 292 (Fig. 1a). This phenomenon is likely associated with the reduction of Fe(III). Towards the end of the reactor operation, a significant increase in the concentration of Fe(II) in the sludge was observed (Fig. 3). This could account for the slight decrease in the ammonium removal after Day230.

Nitrate formation was observed in the effluent, with an average concentration of 16.4 ± 1.1 mg N/L, while nitrite levels remained below 0.5 mg N/L when acetate was absent from the influent (Fig. 1a). The total nitrogen (TN) removal efficiency was only 25.2 ± 1.6 %, significantly lower than the 60.5 % ammonium removal efficiency (Fig. S2). This indicates that approximately 58 % of the removed ammonium was oxidized to nitrate, while the remainder was converted to gas nitrogen components. When organic matter was introduced into the influent, increasing the COD concentration to 50 mg/L, effluent nitrate levels dropped to below 1 mg N/L (Fig. 1a). This change corresponded to a rise in TN removal efficiency to 54.9 % (Fig. 1b), nearly matching the ammonium removal efficiency at the same time. With an influent COD of 100 mg/L during stage III, TN removal efficiency declined to 28.7 ± 9.2 %, mirroring the reduced ammonium removal efficiency. This observation implies that nitrate removal remained effective, potentially facilitated by the addition of organic matter.

The influent phosphate concentration was 6.4 ± 0.27 mg P/L (Fig. 1b). Upon the initial addition of 10 mM amorphous FeOOH on Day 0, the effluent phosphate concentration rapidly decreased to 3.2 mg P/L but gradually increased, stabilizing at a value slightly below the influent concentration (Fig. 1b). Subsequent additions of 10 mM amorphous FeOOH were made on Day 58 and 143. These additions caused rapid decreases in phosphate concentration. Gradual increases to stable levels were observed afterward. The stable levels remained significantly lower than the influent concentration. The stabilized effluent phosphate concentrations were 5.3 ± 0.25, 4.4 ± 0.30, and 3.5 ± 0.41 mg P/L, corresponding to removal efficiencies of 14 %, 33 %, and 50 %, respectively, after the three iron additions. Notably, after the addition of 20 mM amorphous FeOOH on Day 202, the effluent phosphate concentration sharply declined to below 0.5 mg P/L and remained stable at this low level (Fig. 1b), achieving an average phosphate removal efficiency exceeding 90 %. These results suggest that the presence of organic matter significantly enhanced phosphate removal with sufficient addition of iron source. Additionally, through a mass balance of influent and effluent phosphate, it is estimated that approximately 414.6 mg (13.4 mmol) of phosphate has accumulated inside the reactor.

The Feammox bioreactor demonstrated a COD removal efficiency of 94 % at an influent COD concentration of 50 mg/L, and 87 % at an influent COD of 100 mg/L (Fig. 1c), indicating effective organic matter removal.

Furthermore, the average concentrations of dissolved total iron (Fe (T)) and Fe(II) in the effluent were 0.70 ± 0.50 mg/L and 0.34 ± 0.23 mg/L, respectively (Fig. 1d). This corresponds to approximately 77.4 mg (or 1.4 mmol) of iron discharged with the effluent over the 292-day bioreactor operation. Considering the total amount of iron introduced through five amorphous FeOOH additions was 45.6 mmol, the majority (~97 %) of the added iron was retained within the Feammox reactor.

2.2. Batch experiments on nitrate removal

Nitrate removal was further assessed through *ex-situ* batch experiments using Feammox sludge obtained from stage III of the continuous Feammox bioreactor, with varying parameters of nitrate, COD and Fe (II). In the control group (i.e., nitrate addition only), nitrate removal was observed at a rate of 0.70 mg N/(L·h), while nitrite concentrations remained below 1 mg N/L (Figs. 2a and 2b). Soluble COD concentration ranged from 14–21 mg/L (Fig. 2c), despite the absence of added organic matter, and showed no significant decrease during the batch experiments ($p > 0.05$). While soluble Fe(II) concentrations remained below 10 mg/L (Fig. 2d), the total Fe(II) content in the Feammox sludge was approximately 1400 mg/L. These insoluble Fe(II) compounds likely served as the electron donor for nitrate reduction in the absence of other electron donors. These indicates that NDFO potentially contributed to nitrate removal in the control group, independent of organic matter and soluble Fe(II).

The addition of 400 mg/L of soluble Fe(II) enhanced nitrate removal, achieving a rate of 1.25 mg N/(L·h) during the first 9 h (Fig. 2a). Concurrently, soluble Fe(II) concentrations decreased significantly (Fig. 2d), confirming that NDFO facilitated nitrate removal. When organic matter with a COD concentration of approximately 100 mg/L was added, the nitrate removal rate increased to 2.06 mg N/(L·h) during the first 6 h (Fig. 2a). The corresponding decrease in COD (Fig. 2c) indicated that heterotrophic denitrification was responsible for the rapid nitrate removal. Furthermore, the nitrate removal rate via heterotrophic denitrification was faster than that via NDFO when the same COD equivalent of organic matter was compared to Fe(II) (Fig. 2a).

However, there were no significant differences ($p > 0.05$) in the nitrate removal rates between the COD-only group and the COD-Fe(II) group. The Fe(II) concentration also decreased in the COD-Fe(II) group (Fig. 2d), suggesting that both heterotrophic denitrification and NDFO contributed to nitrate removal, with heterotrophic denitrification possibly playing a dominant role.

2.3. Iron accumulation and presence in sludge

The contents of Fe(II) and Fe(III) in the sludge was measured to evaluate the iron reduction and oxidation inside the Feammox reactor. The concentration of Fe(III) in the sludge increased from 74.09 mg/g total suspended solids (TSS) on Day 89 to 95.9 mg/g TSS on Day 129, before decreasing to 42.95 mg/g TSS by Day 292 (Fig. 3). In contrast, the concentration of Fe(II) in the sludge continuously increased from 60.55 mg/g TSS on Day 89 to 150.48 mg/g TSS on Day 292. The Fe(II)/Fe(T) ratio was approximately 45.0 % on Day 89, when no organic matter was added to the influent. This ratio increased to 47.8 % on Day 129 with a COD concentration of 50 mg/L, and further rose to 64.9 % on Day 190 with a COD concentration of 100 mg/L. By Day 292, the Fe(II)/Fe(T) ratio reached 79 %. Therefore, the addition of organic matter to the influent contributed to an increase in the Fe(II)/Fe(T) ratio in sludge.

Additionally, microscopic and scanning electron microscope (SEM) images revealed the presence of Fe(III) compounds and other crystalline structures in the Feammox sludge (Figs. 4a, b, & c). The observed crystals, which shared a similar morphology to those described by Yang et al. (2023) and Deng et al. (2020), suggest the formation of vivianite. The X-ray diffraction (XRD) patterns confirmed the formation of vivianite (Fig. 4d).

2.4. Microbial community analysis

The microbial community in the Feammox bioreactor was analysed to understand the pathways involved in the iron cycle and nitrogen removal (Figure S3). The dominant genera enriched compared to the seed sludge were *norank_f_norank_o_SBR1031* and *norank_f_PHOSHE36*. However, whether these genera play a key role in Feammox, as the functional bacteria involved in this process remains unclear. The relative abundance of *Candidatus_Brocadia,* a dominant genus of anammox bacteria in the seed sludge, significantly decreased from 21.22 % to below 5 %. Another anammox microorganism, *Candidatus_Annamoxoglobus*, exhibited a decline in relative abundance from 0.58 % to undetectable. This suggests a reduction in the anammox activity, mainly because that the operational conditions were not conducive to anammox

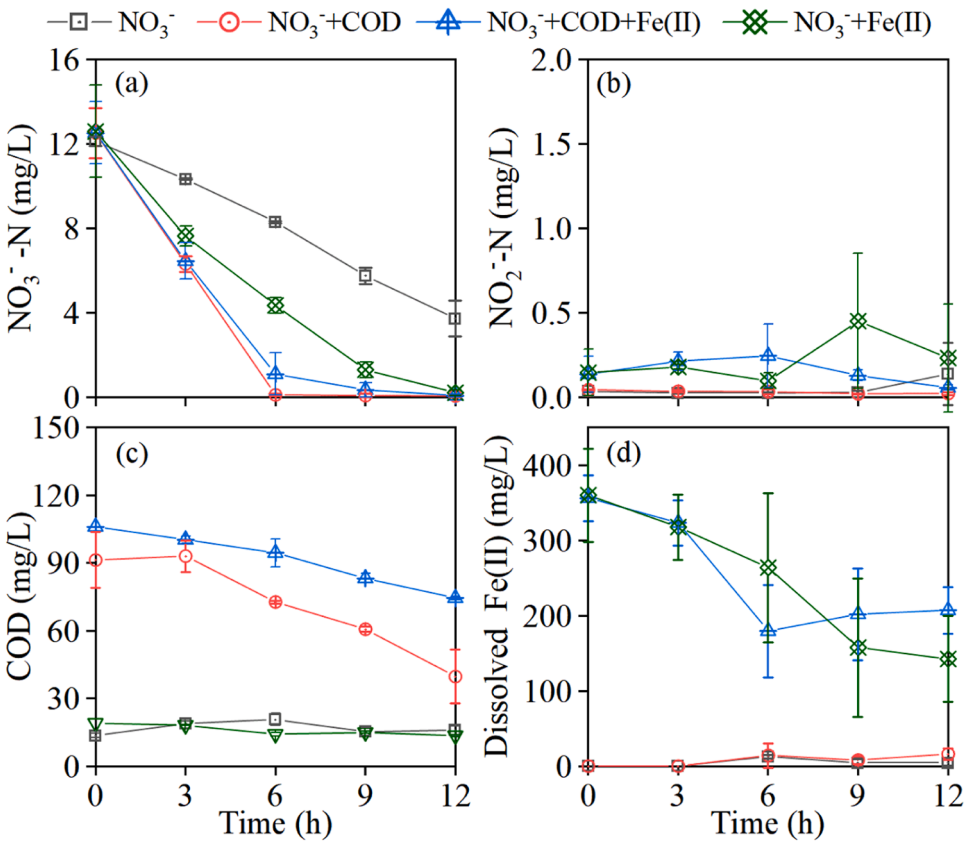

Fig. 2. Variations in concentrations of NO_3^--N (a), NO_2^--N (b), COD (c), and dissolved Fe(II) (d) during *ex-situ* batch experiments.

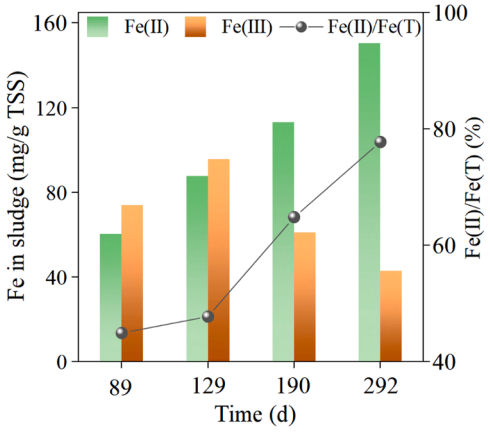

Fig. 3. Concentrations of Fe(II) and Fe(III), and the percentage of Fe(II)/Fe(T) in the sludge samples taken on Days 89, 129, 190, and 292 during the long-term operation of the Feammox bioreactor.

bacteria. Although it still maintained a certain level of relative abundance. This might be due to *Candidatus_Brocadia* utilizing nitrite generated by Feammox for ammonia oxidation, thereby maintaining a stable bacterial population (Ferousi et al., 2017). When organic matter was added to the influent, the nitrite formed from partial denitrification of nitrate could also be utilized by *Candidatus_Brocadia*, facilitating nitrate removal through both denitrification and partial denitrification-anammox processes (Chen et al., 2020).

The anammox seed sludge also contained *Nitrosomonas* and *Nitrospira*, considered ammonia-oxidizing bacteria (AOB) and nitrite-oxidizing bacteria (NOB), respectively. Their relative abundances decreased significantly to below 0.2 % as the reactor operated (Table 1). Only trace amounts of dissolved oxygen (DO < 0.1 mg/L) were present in the reactor. This indicated that the aerobic ammonia oxidation rate was extremely low and negligible. Thus, it suggested that Feammox was the primary pathway for ammonia oxidation.

Even though there have been many studies on Feammox, there is still a lack of clear conclusions on whether there exists a class of Feammox functional bacteria. Recent research highlighted potential functional microorganisms involved in Feammox, identifying *Subgroup_10* and *Paludibaculum* as candidates (Jia et al., 2025). In this study, the relative abundances of these two microorganisms also increased, although they remained relatively low (< 0.3 %). Many studies have found that iron reducing bacteria play an important role in the Feammox process (Li et al., 2015; Zhou et al., 2016). Genera such as *Geobacter* (Guo et al., 2023), *Desulfomicrobium, Dechloromonas* (Zhang et al., 2022), *Bacillus, Comamonas, Geothrix* (Wang et al., 2014), *Citrifermentans* (Zhang et al., 2023b), *Acinetobacter*, and *Ferruginibacter* (Hao et al., 2024) detected in this study are typical iron-reducing bacteria. Although their relative abundance was low, the total abundance of iron-reducing bacteria increased from 0.007 % in the seed sludge to 1.592 % on Day 292 (Table 1). This suggests that the domestication of Feammox functionality led to the enrichment of iron-reducing bacteria.

Moreover, the total relative abundances of iron-oxidizing bacteria, including *unclassified_f_Gallionellaceae* (Bethencourt et al., 2020), *Rhodanobacter* (Hao et al., 2024), and *Thiobacillus* (Kanaparthi and Conrad, 2015), was 0.069 % in the seed sludge, increasing to 0.452 % on Day 89, indicating the presence of the NDFO process. However, after the addition of organic matter to the influent, the relative abundance of these iron-oxidizing bacteria continued to decrease, reaching 0.124 % on Day 292. The decrease in the abundance of microorganisms involved in nitrate reduction was likely attributed to the diminished nitrate production as a Feammox byproduct, which would restrict the supply of substrates required for their metabolic activity.

In addition, *Denitratisoma*, which has been reported to be closely

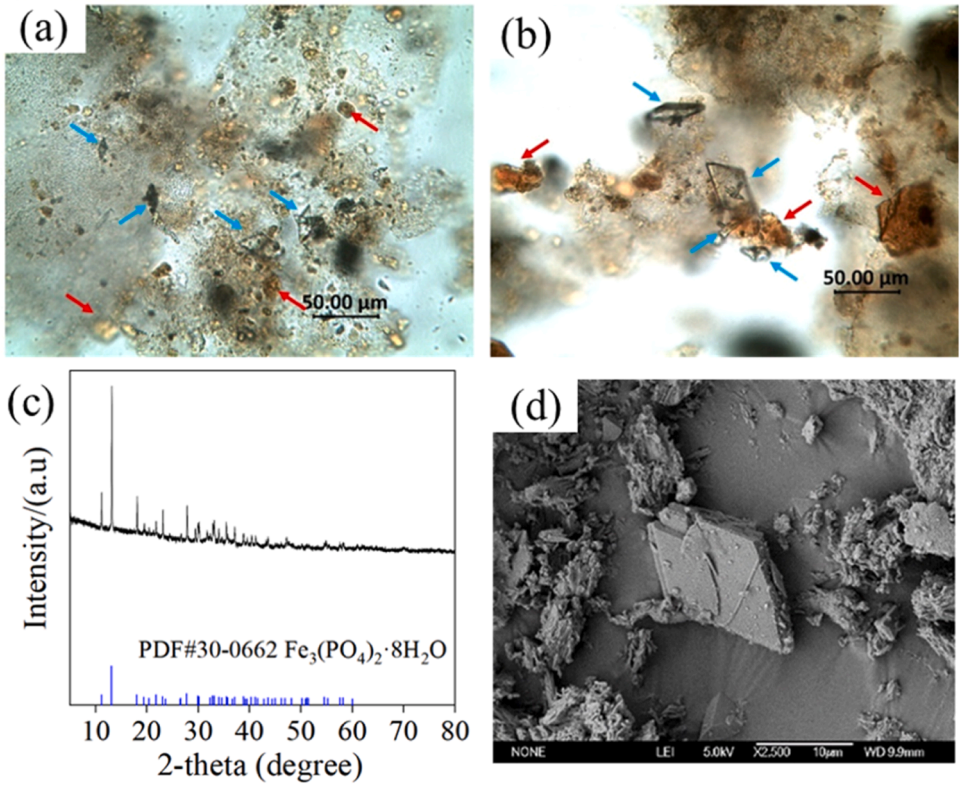

Fig. 4. Microscopic images of solid products obtained from the Feammox bioreactor on Day 58 (a) and Day 203 (b), with blue arrows indicating vivianite and red arrows indicating Fe(III) compounds. (c) SEM image and (d) XRD patterns of the sludge obtained on Day 203.

Table 1
Relative abundances (%) of typical bacteria at the genus level in the Feammox bioreactor.

Bacteria	Genera	Day 0	Day 89	Day 139	Day 292
Anammox bacteria	*Candidatus_Brocadia*	21.22	6.37	4.4	4.82
	Candidatus_Annamoxoglobus	0.58	0	0	0
AOB	*Nitrosomonas*	1.53	0.21	0.13	0.06
NOB	*Nitrospira*	4.98	0.14	0.12	0.01
	In total	28.31	6.72	4.65	4.87
Fe(III) reduction bacteria	*Geobacter*	0	0	0	0.022
	Desulfomicrobium	0	0.027	0.03	0.01
	Dechloromonas	0	0.072	0.04	0.272
	Bacillus	0	0.017	0.045	0.02
	Comamonas	0.007	0.206	0.243	1.07
	Citrifermentans	0	0.201	0.124	0.146
	Geothrix	0	0.012	0.01	0.002
	Acinetobacter	0	0	0.139	3.215
	Ferruginibacter	0	0.154	0.092	0.05
	In total	0.007	0.689	0.584	1.592
Fe(II) oxidation bacteria	*Gallionellaceae*	0	0.253	0.124	0
	Rhodanobacter	0	0.05	0.01	0.027
	Thiobacillus	0.069	0.149	0.134	0.097
	In total	0.069	0.452	0.268	0.124

associated with NDFO (Zhang et al., 2023a), showed an increase in the relative abundance from 2.93 % at the beginning to 4.24 % towards the end of stage I. This increase was likely due to the nitrate production through Feammox, which provided substrates for its metabolism. However, following the introduction of organic matter, its relative abundance decreased to 3.82 % by the end of the reactor operation, presumably due to the effective removal of nitrate.

With the increase in the organic matter concentration, the abundance of *Luteimonas* at the genus level was 0, 0.0025 %, and 0.012 % in stages I, II, and III, respectively. Similarly, the abundance of *Comamonas* increased from 0.007 % to 0.24 % and 1.06 %, while *Hydrogenophaga* increased from 0 to 0.047 % and 0.91 %. Previous studies have identified these bacteria as capable of performing heterotrophic or mixotrophic denitrification (Jang et al., 2024), which might explain their progressive increase in their abundances. However, many microorganisms associated with dissimilatory iron reduction also could utilize organic matter as electron donor for iron reduction. As a result, the overall abundances of these iron-metabolizing microorganisms tended to increase with the increasing organic matter concentration.

3. Discussion

This study is the first to reveal the role of organic matter in Feammox-driven nitrogen and phosphorus removal. Organic matter in the influent negatively impacted ammonium removal, likely due to (1) the inhibition effect of organic matter on the ammonia oxidation efficiency in Feammox and (2) heterotrophic dissimilatory iron reduction outcompeting Feammox for Fe(III) (Li et al., 2015; Zhou et al., 2016). Theoretically, dissimilatory iron reduction occurs more preferentially than Feammox because of its lower standard Gibbs free energy (−1410−−1330 kJ/mol) (Lovley and Phillips, 1987), which could be the main reason for the inhibition of Feammox by organic matter. This is consistent with the previous findings (Ma et al., 2022; Nguyen et al., 2023; Zhu et al., 2022). However, Feammox systems, inoculated with anaerobic sludge adapted to high organic load wastewater, have shown strong resistance to organic matter inhibition and even enhanced ammonium removal (Le et al., 2021; Liang et al., 2023). This might be due to that the Feammox process was coupled with heterotrophy or appropriate content of organic matter was essential for the microbial

community in Feammox. However, this study demonstrates that Feammox reactors seeded with anammox sludge are more sensitive to organic matter content.

Conversely, organic matter significantly enhanced nitrate removal, predominantly through heterotrophic denitrification rather than nitrate-dependent Fe(II) oxidation (NDFO) (Fig. 2). This finding underscores the competitive advantage of heterotrophic denitrification over NDFO in environments with sufficient organic carbon availability.

Phosphorus removal in the Feammox reactor was also improved with the addition of organic matter. Initially, phosphate removal was driven by adsorption onto amorphous FeOOH, a known effective phosphate adsorbent (Belloni et al., 2023; Zhang et al., 2021). Over time, however, the adsorption sites became saturated, causing the equilibrium concentration of phosphate to gradually rise, a trend consistent with breakthrough behaviour in adsorption systems (Ajmal et al., 2018; Dorau et al., 2019). Despite this, the effluent phosphate concentration remained consistently lower than the influent level. This sustained removal can be attributed to the precipitation of Fe(II) with phosphate, forming insoluble vivianite crystals, as confirmed by XRD analysis (Fig. 4d). The availability of Fe(II), produced through dissimilatory iron reduction, was significantly enhanced following the addition of organic matter (Fig. 3).

Interestingly, methane was not detected in the headspace of the Feammox reactor throughout the study. This suggests that organic matter was not consumed by methanogenic processes, which convert organic carbon into methane and carbon dioxide (Siddique and Wahid, 2018). The absence of methane is likely due to the significant availability of competing electron acceptors (Keller et al., 2023), such as nitrate from Feammox and Fe(III), which suppressed methanogenic activity.

Moreover, the addition of an extensive iron source on Day 202 appeared to mitigate the inhibitory effect of organic matter on ammonia oxidation. This improvement coincided with an increase in the Fe(II)/Fe(T) ratio in the sludge, which rose from 65 % on Day 190 to 79 % on Day 292 (Fig. 3). This indicates that the supplemented Fe(III) acted as an electron acceptor, allowing organic matter to be consumed and reducing its inhibitory effect. Additionally, the added Fe(III) enhanced the overall performance of the Feammox reactor, a key electron acceptor required for Feammox performance.

This study highlights the sensitivity of Feammox-derived nitrogen and phosphorus removal to the presence of organic matter in the influent. Managing the balance of organic matter is critical for optimizing Feammox performance on nitrogen and phosphorus removal. A pretreatment step to remove excessive organic matter may be necessary to minimize its inhibitory impact on ammonium removal. However, residual organic matter remains beneficial for nitrate and phosphorus removal, as it facilitates heterotrophic denitrification and enhances Fe(II)-mediated phosphate precipitation. These findings underscore the dual role of organic matter and the need for a balanced approach to optimize Feammox performance for simultaneous nitrogen and phosphorus removal.

In general, Feammox is particularly suitable for treating domestic wastewater with low organic matter. However, even low concentrations of organic matter can lead to an increase in iron source consumption. To reduce the operation cost, iron sources could include waste-derived materials, such as scrap iron or Fenton sludge, promoting waste recycling and resource recovery. For wastewater with normal or high organic loads, a multi-stage system can be proposed to remove organic matter in the initial stage, minimizing its inhibitory effects on Feammox in the subsequent stage. Particularly, organics in sewage is an important bioenergy resource for recovery (Abdelrahman et al., 2023). Recovering the energy provides good opportunity for net-zero emissions (Gandiglio et al., 2017). Then, coupling of the bioenergy recovery process and Feammox would provide an opportunity to create a next-generation wastewater treatment technology.

4. Conclusions

This study revealed the role of organic matter in Feammox-driven nitrogen and phosphorus removal. The ammonia oxidation was inhibited by organic matter, likely due to competition with iron reducing bacteria for Fe(III). Moreover, organic matter enhanced the removal of nitrate formed in Feammox and promoted phosphorus removal via Fe(II)-mediated vivianite precipitation. The addition of supplemental iron would promote the growth of iron reducing bacteria, which in turn would increase the organic matter consumption rate. As a result, the inhibition effect of organic matter on Feammox would be alleviated to some extent, thereby improving system performance. These findings highlight the need for balancing organic matter levels to optimize Feammox systems for simultaneous nitrogen and phosphorus removal in wastewater treatment.

5. Materials and methods

5.1. Synthetic wastewater and iron source

The synthetic wastewater used in the present study was prepared by 191.03 mg/L NH_4Cl, 200 mg/L $MgCl_2{\cdot}6H_2O$, 136 mg/L $CaCl_2{\cdot}2H_2O$, 27 mg/L KH_2PO_4, 500 mg/L $NaHCO_3$, and 1 mL/L micronutrient solution (the detailed composition in Text S1). CH_3COONa was added in the synthetic wastewater as organic matter when needed. The synthetic wastewater was aerated with a mixed gas of N_2/CO_2 (80 %/20 %), and the concentration of DO was maintained below 0.1 mg/L. Amorphous FeOOH was used as the iron source for Feammox. The specific preparation method can be found in Text S2.

5.2. Reactor set-up and long-term experimental procedure

An up-flow Feammox reactor (total volume of 1.2 L) was used for long-term operation (Figure S1). The inner diameter and effective height were 9 cm and 12 cm, respectively, with a working volume of 0.76 L. The influent was pumped into the reactor from the bottom using a peristaltic pump (BT100–2 J, Longer Pump, China), and the effluent was discharged from the top outlet, which was connected to an S-bend pipe to prevent air from entering the reactor. A three-phase separator was employed in the reactor to extract gas and separate sludge particles from the effluent. Additionally, the reactor was covered with aluminum foil to prevent photochemical reactions.

The Feammox reactor was started by inoculating it with anammox granular sludge obtained from a local pilot anammox reactor. The pilot-scale anammox reactor had been operated for >3 years, achieving effective nitrogen removal. During domestication, an initial dose of 10 mM amorphous FeOOH to anammox sludge. The ammonia removal efficiency increased and stabilized over 30 days. Afterward, the reactor was continuously operated for approximately 300 days to investigate the effect of organic matter on Feammox, with a hydraulic retention time (HRT) of 2 days. The concentration of TSS in the Feammox reactor was 15.5–18.1 mg/L. During the operation, amorphous FeOOH was further added to the reactor on day 58 and 143 at a dosage of 10 mM, and on day 202 at a dosage of 20 mM. The reactor was operated at room temperature. The influent and the effluent samples were taken regularly and immediately filtered using a filter equipped with a polyether sulphone membrane with pore size of 0.45 μm (TGMF60, Jinteng, China) before analysis. The overall operation of the reactor is divided into three stages based on changes in organic matter. Stage I (0–95 days) had a COD concentration of 0 mg/L and stage II (96–145 days) had a COD concentration of 50 mg/L. Stage III (100 mg COD/L) is further subdivided into two stages, i.e. stage III-A (146–201 days) and stage III-B (202–292 days). In this study, the C/N ratio is defined as a mass ratio of COD concentration (mg/L) to influent ammonium concentration (mg N/L).

5.3. Ex-situ batch experiments

Ex-situ batch experiments were conducted to identify the pathways contributing to nitrate removal, specifically heterotrophic denitrification and NDFO. A certain amount of sludge obtained during the stage III-B of bioreactor operation was washed three times with deionized water to remove residual substrates and then evenly distributed into several 100 mL serum bottles. Each bottle was filled with 70 mL of synthetic wastewater, resulting in an average TSS concentration of 8660 mg/L. CH_3COONa was added as the organic matter for heterotrophic denitrification, while $FeSO_4{\cdot}7H_2O$ served as the Fe(II) source for NDFO. The dosages of CH_3COONa and $FeSO_4{\cdot}7H_2O$ were determined based on the assumption that they could provide equivalent electrons for nitrate reduction. The mixed liquors contained in the bottles were deaerated by N_2/CO_2 (80 %/20 %) gas sparging for 30 min and then sealed with butyl rubber stoppers and capped with aluminum caps. To further eliminate residual oxygen in the headspace, two hypodermic needles were inserted into each bottle, one as the gas inlet and the other as the outlet, and the bottles were flushed with N_2 for 10 min. The oxygen-free bottles were then cultivated in a shaker (THZ-98C, YiHeng, China) at 120 rpm and 25 ℃. All experiments were conducted in triplicate. Details of the specific conditions are summarized in Table 2.

5.4. Analysis methods

The solution pH and DO were determined by a laboratory pH meter (Leici E−301F, Shanghai INESA & Scientific Instrument, China) and a DO meter (Oxi3310, WTW, Germany). The COD, ammonium, nitrite, nitrate, Fe(II) and total Fe in aquatic samples were measured colorimetrically in an ultraviolet spectrophotometer (DR 3900, HACH, USA) according to standard methods (APHA, 2017). Fe(II) and total Fe in sludge sample (1 mL) was extracted with 5 mL of 3.6 M HCl solution for 16 h at room temperature before analysis, and the concentration of Fe (III) was calculated as the conference difference between total Fe and Fe (II).

For TSS measurements, samples were dried under 105 °C for 2 h after filtration (0.7 μm, Ashless 1441–55, Whatman, UK) and then TSS was calculated by the weight difference divided by the sample volume. Sludge samples were examined using a digital microscope (Smart 320, Optec, China). An SEM (JEOL, JSM-6700F, Japan) equipped with an energy dispersive spectroscopy detector was employed to observe the morphology and the elemental composition of sludge and solid precipitates. XRD analysis was conducted using a diffractometer (XRD-7000, Shimazu, Japan) by applying Cu Kα radiation (40 kV, 40 mA) at a scanning rate of 5°/min.

The removal efficiencies of ammonia, TN, phosphate, and COD were calculated from the influent and effluent concentrations. The concentration of TN was not directly measured in this study, but was estimated as the sum of nitrogen concentrations in ammonia, nitrite, and nitrate.

5.5. Microbial community analysis

The sludge sample was mixed at 500 rpm by a magnetic stirrer (RCT B S025, IKA, Germany) equipped on the reactor bottom, and then 10 mL of the sludge was sampled which was frozen at −20 °C (BCD-309, Haier, China). The frozen sludge sample was used for high-throughput sequencing analysis by Majorbio Bio-Pharm Technology Ltd. (Shanghai, China). Deoxyribonucleic acid (DNA) was extracted from the sludge sample using the rapid DNA soil rotation kit (Omega Bio-Tek, Inc., USA). The V3–V4 region of the bacterial 16S ribosomal ribonucleic acid was amplified with primer 338F-806R. Sequencing of the polymerase chain reaction products was conducted on an Illumina MiSeq PE300 platform (Illumina, USA). The data were analyzed on the free online platform of Majorbio Platform (www.majorbio.com).

Table 2
Specific conditions of the *ex-situ* batch experiments.

Serial No.	Nitrate (mg N/L)	COD (mg/L)	Fe(II) (mg/L)	Condition
B1	10	0	0	Biotic
B2	10	100	0	Biotic
B3	10	100	400	Biotic
B4	10	0	400	Biotic

CRediT authorship contribution statement

Yi Liu: Writing – original draft, Visualization, Methodology, Investigation, Data curation, Conceptualization. **Jiachen Dong:** Investigation, Data curation. **Xiaohui Cheng:** Investigation, Data curation. **Xiaotong Cen:** Writing – review & editing, Validation. **Yan Dang:** Writing – review & editing, Validation. **Kangning Xu:** Writing – review & editing, Validation, Supervision, Resources, Project administration, Conceptualization. **Min Zheng:** Writing – review & editing, Validation, Conceptualization.

Declaration of competing interest

The authors declare that they have no known competing financial interests or personal relationships that could have appeared to influence the work reported in this paper.

Acknowledgments

This study is financially supported by the National Natural Science Foundation of China (No. 52270022) at Beijing Forestry University. Min Zheng acknowledges the support of the Australian Research Council Industry Fellowship (IE230100245) and Linkage Project (LP230201054).

Supplementary materials

Supplementary material associated with this article can be found, in the online version, at doi:10.1016/j.wroa.2025.100312.

Data availability

Data will be made available on request.

References

Abdelrahman, A.M., Kosar, S., Gulhan, H., Cicekalan, B., Ucas, G., Atli, E., Guven, H., Ozgun, H., Ozturk, I., Koyuncu, I., van Lier, J.B., Volcke, E.I.P., Ersahin, M.E., 2023. Impact of primary treatment methods on sludge characteristics and digestibility, and wastewater treatment plant-wide economics. Water Res. 235, 119920.

Ajmal, Z., Muhmood, A., Usman, M., Kizito, S., Lu, J., Dong, R., Wu, S., 2018. Phosphate removal from aqueous solution using iron oxides: adsorption, desorption and regeneration characteristics. J. Colloid Interface Sci. 528, 145–155.

APHA, 2017. Standard Methods For the Examination of Water and Wastewater, 23rd ed. American Public Health Association, Washington, D.C, USA.

Belloni, C., Korving, L., Witkamp, G.J., Brück, E., de Jager, P., Dugulan, A.I., 2023. FeOOH and (Fe, Zn)OOH hybrid anion exchange adsorbents for phosphate recovery: a determination of Fe-phases and adsorption–desorption mechanism. Chem. Eng. J. (Basel) 473, 145287.

Bethencourt, L., Bochet, O., Farasin, J., Aquilina, L., Borgne, T.L., Quaiser, A., Biget, M., Michon-Coudouel, S., Labasque, T., Dufresne, A., 2020. Genome reconstruction reveals distinct assemblages of *Gallionellaceae* in surface and subsurface redox transition zones. FEMS Microbiol. Ecol. 96 (5), fiaa036.

Chen, W., Chen, S., Hu, F., Liu, W., Yang, D., Wu, J., 2020. A novel anammox reactor with a nitrogen gas circulation: performance, granule size, activity, and microbial community. Environ. Sci. Pollut. Res. 27 (15), 18661–18671.

Cheng, X., Hu, L., Liu, T., Cheng, X., Li, J., Xu, K., Zheng, M., 2025. High-level nitrogen removal achieved by Feammox-based autotrophic nitrogen conversion. Water Res. X 27, 100292.

Clément, J., Shrestha, J., Ehrenfeld, J.G., Jaffé, P.R., 2005. Ammonium oxidation coupled to dissimilatory reduction of iron under anaerobic conditions in wetland soils. Soil Biol. Biochem. 37 (12), 2323–2328.

Deng, S., Zhang, C., Dang, Y., Collins, R.N., Kinsela, A.S., Tian, J., Holmes, D.E., Li, H., Qiu, B., Cheng, X., Waite, T.D., 2020. Iron transformation and its role in phosphorus

immobilization in a UCT-MBR with vivianite formation enhancement. Environ. Sci. Technol. 54 (19), 12539–12549.
Ding, B., Li, Z., Qin, Y., 2017. Nitrogen loss from anaerobic ammonium oxidation coupled to iron(III) reduction in a riparian zone. Environ. Pollut. 231, 379–386.
Ding, L., An, X., Li, S., Zhang, G., Zhu, Y., 2014. Nitrogen loss through anaerobic ammonium oxidation coupled to iron reduction from paddy soils in a chronosequence. Environ. Sci. Technol. 48 (18), 10641–10647.
Dorau, K., Pohl, L., Just, C., Höschen, C., Ufer, K., Mansfeldt, T., Mueller, C.W., 2019. Soil organic matter and phosphate sorption on natural and synthetic Fe oxides under in situ conditions. Environ. Sci. Technol. 53 (22), 13081–13087.
Ferousi, C., Lindhoud, S., Baymann, F., Kartal, B., Jetten, M.S., Reimann, J., 2017. Iron assimilation and utilization in anaerobic ammonium oxidizing bacteria. Curr. Opin. Chem. Biol. 37, 129–136.
Gandiglio, M., Lanzini, A., Soto, A., Leone, P., Santarelli, M., 2017. Enhancing the energy efficiency of wastewater treatment plants through co-digestion and fuel cell systems. Front. Environ. Sci. 5, 70.
Guo, W., Ying, X., Zhao, N., Yu, S., Zhang, X., Feng, H., Zhang, Y., Yu, H., 2023. Interspecies electron transfer between *Geobacter* and denitrifying bacteria for nitrogen removal in bioelectrochemical system. Chem. Eng. J. (Basel) 455, 139821.
Hao, X., Zeng, W., Li, J., Zhan, M., Miao, H., Gong, Q., 2024. High-efficient nitrogen removal with low demand of Fe source and mechanism analysis driven by Fe(II)/Fe (III) cycle. Chem. Eng. J. (Basel) 481, 148702.
Hu, L., Cheng, X., Qi, G., Zheng, M., Dang, Y., Li, J., Xu, K., 2022. Achieving ammonium removal through anammox-derived Feammox with low demand of Fe(III). Front. Microbiol. 13, 918634.
Jang, Y., Lee, S., Kim, N., Park, H., 2024. Metagenomic analysis reveals abundance of mixotrophic, heterotrophic, and homoacetogenic bacteria in a hydrogen-based membrane biofilm reactor. Water Res. 267, 122564.
Jia, F., Chen, Y., Xu, Z., Gao, X., Mei, N., Qi, X., Yang, L., Jiang, J., Hou, L., Yao, H., 2025. FeO might be more suitable than Fe^{2+} for the construction of anammox-dominated Fe-N coupling system: based on ^{15}N isotope tracing. Water Res. 274, 123097.
Kanaparthi, D., Conrad, R., 2015. Role of humic substances in promoting autotrophic growth in nitrate-dependent iron-oxidizing bacteria. Syst. Appl. Microbiol. 38 (3), 184–188.
Keller, J.K., Bridgham, S.D., Takagi, K.K., Zalman, C.A., Rush, J.E., Anderson, C., Mosolf, J.M., Gabriel, K.N., 2023. Microbial organic matter reduction regulates methane and carbon dioxide production across an ombrotrophic-minerotrophic peatland gradient. Soil Biol. Biochem. (Basel) 182, 109045.
Le, C.P., Nguyen, H.T., Nguyen, T.D., Nguyen, Q.H.M., Pham, H.T., Dinh, H.T., 2021. Ammonium and organic carbon co-removal under feammox-coupled-with-heterotrophy condition as an efficient approach for nitrogen treatment. Sci. Rep. 11 (1), 784.
Li, X., Hou, L., Liu, M., Zheng, Y., Yin, G., Lin, X., Cheng, L., Li, Y., Hu, X., 2015. Evidence of nitrogen loss from anaerobic ammonium oxidation coupled with ferric iron reduction in an intertidal wetland. Environ. Sci. Technol. 49 (19), 11560–11568.
Li, X., Huang, Y., Liu, H., Wu, C., Bi, W., Yuan, Y., Liu, X., 2018. Simultaneous Fe(III) reduction and ammonia oxidation process in Anammox sludge. J. Environ. Sci. 64, 42–50.
Liang, E., Xu, L., Su, J., Liu, Y., Qi, S., Li, X., 2023. Hydrogel bioreactor drives feammox and synergistically removes composite pollutants: performance optimization, microbial communities and functional genetic differences. Bioresour. Technol. 387, 129604.
Lovley, D.R., Phillips, E.J.P., 1987. Competitive mechanisms for inhibition of sulfate reduction and methane production in the zone of ferric iron reduction in sediments. Appl. Environ. Microbiol. 53 (11), 2636–2641.
Ma, D., Wang, J., Li, H., Che, J., Yue, Z., 2022. Simultaneous removal of COD and NH_4^+-N from domestic sewage by a single-stage up-flow anaerobic biological filter based on Feammox. Environ. Pollut. 314, 120213.
Nguyen, H.T., Nguyen, L.D., Le, C.P., Hoang, N.D., Dinh, H.T., 2023. Nitrogen and carbon removal from anaerobic digester effluents with low carbon to nitrogen ratios under feammox conditions. Bioresour. Technol. 371, 128585.
Siddique, M.N.I., Wahid, Z.A., 2018. Achievements and perspectives of anaerobic co-digestion: a review. J. Clean. Prod. 194, 359–371.
Struab, K.L., Benz, M., Schink, B., Widdel, F., 1996. Anaerobic, nitrate-dependent microbial oxidation of ferrous iron. Appl. Environ. Microbiol. 62 (4), 1458–1460.
Wang, G., Chen, T., Yue, Z., Zhou, Y., Wang, J., 2014. Isolation and characterization of *Pseudomonas stutzeri* capable of reducing Fe(III) and nitrate from skarn-type copper mine tailings. Geomicrobiol. J. 31 (6), 509–518.
Wang, J., Song, C., Huo, L., Wang, X., Liu, H., Zhang, X., 2024. Nitrogen removal performance and thermodynamic mechanisms of feammox mediated by Ferric pyrophosphate at various pHs. J. Water. Process. Eng. 58, 104864.
Xing, W., Li, J., Li, D., Hu, J., Deng, S., Cui, Y., Yao, H., 2018. Stable-isotope probing reveals the activity and function of autotrophic and heterotrophic denitrifiers in nitrate removal from organic-limited wastewater. Environ. Sci. Technol. 52 (14), 7867–7875.
Yang, W.H., Weber, K.A., Silver, W.L., 2012. Nitrogen loss from soil through anaerobic ammonium oxidation coupled to iron reduction. Nat. Geosci. 5 (8), 538–541.
Yang, X., Zhang, C., Zhang, X., Deng, S., Cheng, X., Waite, T.D., 2023. Phosphate recovery from aqueous solutions via vivianite crystallization: interference of Fe^{II} oxidation at different do concentrations and pHs. Environ. Sci. Technol. 57 (5), 2105–2117.
Yang, Y., Zhang, Y., Li, Y., Zhao, H., Peng, H., 2018. Nitrogen removal during anaerobic digestion of wasted activated sludge under supplementing Fe(III) compounds. Chem. Eng. J. 332, 711–716.
Zhang, L., Li, W., Li, J., Wang, Y., Xie, H., Zhao, W., 2022. A novel iron-mediated nitrogen removal technology of ammonium oxidation coupled to nitrate/nitrite reduction: recent advances. J. Environ. Manage. 319, 115779.
Zhang, X., Yao, H., Lei, X., Lian, Q., Roy, A., Doucet, D., Yan, H., Zappi, M.E., Gang, D.D., 2021. A comparative study for phosphate adsorption on amorphous FeOOH and goethite (α-FeOOH): an investigation of relationship between the surface chemistry and structure. Environ. Res. 199, 111223.
Zhang, Y., Ji, S., Xie, P., Liang, Y., Chen, H., Chen, L., Wei, C., Yang, Z., Qiu, G., 2023a. Simultaneous partial nitrification, anammox and nitrate-dependent Fe(II) oxidation (NDFO) for total nitrogen removal under limited dissolved oxygen and completely autotrophic conditions. Sci. Total Environ. 880, 163300.
Zhang, Y., O'Loughlin, E.J., Park, S., Kwon, M.J., 2023b. Effects of Fe(III) (hydr)oxide mineralogy on the development of microbial communities originating from soil, surface water, groundwater, and aerosols. Sci. Total Environ. 905, 166993.
Zhen, J., Zheng, M., Wei, W., Ni, S.-Q., Ni, B.-J., 2024. Extracellular electron transfer (EET) dependent anammox process for progressive nitrogen removal: a critical review. Chem. Eng. J. 482, 148886.
Zheng, M., Lloyd, J., Wardrop, P., Duan, H., Liu, T., Ye, L., Ni, B.-J., 2025. Path to zero emission of nitrous oxide in sewage treatment: is nitrification controllable or avoidable? Curr. Opin. Biotechnol. 91, 103230.
Zhou, G., Yang, X., Li, H., Marshall, C.W., Zheng, B., Yan, Y., Su, J., Zhu, Y., 2016. Electron shuttles enhance anaerobic ammonium oxidation coupled to iron(III) reduction. Environ. Sci. Technol. 50 (17), 9298–9307.
Zhu, T., Lai, W., Zhang, Y., Liu, Y., 2022. Feammox process driven anaerobic ammonium removal of wastewater treatment under supplementing Fe(III) compounds. Sci. Total Environ. 804, 149965.